Journal of
Materials Chemistry A

Accepted Manuscript

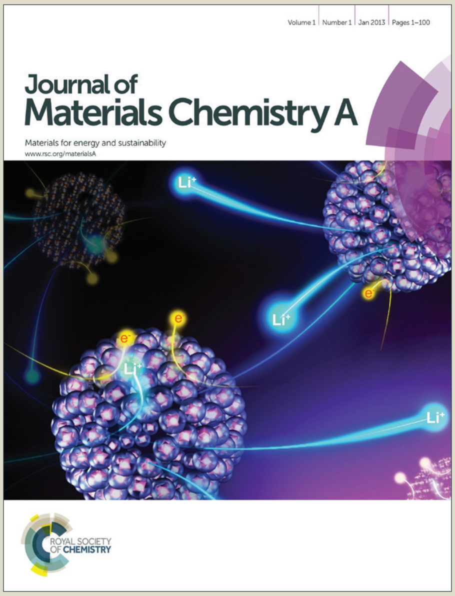

ROYAL SOCIETY
OF **CHEMISTRY**

www.rsc.org/materialsA

Journal Name

ARTICLE

Anion-effect on electrochemical properties of ionic liquid electrolytes for rechargeable aluminum batteries

Received 00th January 20xx,
Accepted 00th January 20xx

DOI: 10.1039/x0xx00000x

www.rsc.org/

Huali Wang, [a] Sichen Gu, [a] Ying Bai, [a,**] Shi Chen, [a, b] Na Zhu, [a] Chuan Wu, [a,b**] and Feng Wu [a, b]

Rechargeable aluminum battery is considered as a promising battery system used in energy storage devices, due to its abundant natural resources and high capacity. However, fabrication of this battery working at room temperature didn't succeed until haloaluminate containd ionic liquids were used as electrolytes. Therefore, anions are expected to have a great effect on performance of rechargeable aluminum battery. For a fully understanding of anion-effect, haloaluminate containd ionic liquids prepared with different halogenated imidazole salt and $AlCl_3$/imidazolium chloride mole ratio are studied. Electrochemical window is found narrowing with reducibility of halide ion, which is confirmed by caclulation result using density functional theory (DFT) method. For ionic liquids at different mole ratio, the coexistance of different chloroaluminate anions (Cl^-, $AlCl_4^-$, $Al_2Cl_7^-$) is found. When used as electrolyte in rechargeable aluminum battery with V_2O_5 nanowire cathode, $AlCl_3$/[BMIM]Cl ionic liquid with the mole ration of 1.1:1 shows the best performance. The as-assembled cell exhibits a high discharge voltage platform (1 V) and capacity (288 mAh/g) at the first cycle. Concentration of $Al_2Cl_7^-$ is considered as a key factor in chloroaluminate ionic liquids when used as electrolyte. Furthermore, a slightly corrosion is found on the surface of Al metal foil immerged in $AlCl_3$/[BMIM]Cl=1.1:1 ionic liquid for 24h, which may help removing the oxide film on Al metal foil, so as to improve the charge/discharge performance.

Introduction

As increasing amounts of electric power are derived from natural sources (solar, wind), transformational storage technologies become ever more important. Therefore, development of new battery systems using abundant natural resources, such as Na-ion[1-6], Mg-ion[7-11] and Al-ion batteries[12-23], is urgently needed in stationary battery for uninterrupted electricity and load levelling as well as grid energy storage systems. As an emerging battery system, rechargeable aluminum battery with a three electron redox couples has a distinct advantage in its capacity and the potential to increase the energy density of a cell by several orders of magnitude[24-26]. However, research of rechargeable aluminum battery working at room temperature was at a standstill until ionic liquids were used as electrolytes. This aroused great interest among researchers.

The standard reduction potential of Al^{3+} (-1.68 V vs. standard hydrogen electrode) is lower than that of hydrogen evolution reaction in an aqueous solutions. Rechargeable aluminum batteries using aqueous solution electrolyte are unavoidable accompanied by hydrogen evolution reaction, which can't be used in a closed system[17, 18]. Thus, electrolyte consisting of Al salt and organic solvents were investigated[27]. However, no charge/discharge performance of battery using such electrolyte is given. Room Temperature Ionic Liquids (RTILs)[28-30] with wide electrochemical window and high conductivity have been widely used in secondary batteries recent year. Rechargeable aluminum batteries adopted $AlCl_3$ containing imidazolium ionic liquids ($AlCl_3$/[BMIM]Br, $AlCl_3$/[BMIM]Cl, $AlCl_3$/[EMIM]Cl) as electrolyte showed very stable electrochemical behavior[12-16, 19].

Choosing a right electrolyte is important for successful battery technology. $AlCl_3$ containing ionic liquids were used in rechargeable aluminum batteries as a priority, since no additional Al salts are necessary in these electrolytes. Haloaluminate anions act as the electrochemical active substance. Hence, anions may have a great effect on electrochemical properties of ionic liquids, as well as battery performance. Though different ionic liquids have been used in rechargeable aluminum batteries, no research revealed the effect brought by anions, and give a clear description on relationship between anions and electrochemical properties. A fully understanding of these ionic liquids can help us choose and optimize electrolyte properly in the future. In this paper, effect of anions on properties of ionic liquids and battery performance are investigated, by preparing $AlCl_3$ imidazolium ionic liquids with different halogenated imidazole salt and $AlCl_3$/imidazolium chloride mole ratio. Meanwhile density functional theory (DFT) calculation is conducted to explore structure-function relationship of ionic liquids.

---

a Beijing Key Laboratory of Environmental Science and Engineering, School of Materials Science & Engineering, Beijing Institute of Technology, Beijing 100081, China. E-mail: Y. Bai (membrane@bit.edu.cn), C. Wu (chuanwu@bit.edu.cn)
b Collaborative Innovation Center of Electric Vehicles in Beijing, Beijing 100081, China

Experimental

Ionic liquid preparation and battery assembly

Three kinds of halogenated imidazole salt (1-butyl-3-methylimidazolium chloride ([BMIM]Cl), 1-butyl-3-methylimidazolium bromide ([BMIM]Br) and 1-butyl-3-methylimidazolium iodide ([BMIM]I)) and $AlCl_3$ (bought from Alfa Aesar)were used as received. Ionic liquids were prepared in a glove box filled with dry argon by mixing $AlCl_3$ with halogenated imidazole salt according to designed molar ratio. The reactants were stirred overnight until homogeneous and clear liquid obtained.

To investigate anion-effect on battery performance, rechargeable aluminum batteries (2025 coin-type cells) were assembled in an argon-filled glove box (MBraun Labmaster130). The cathode was made with V_2O_5 nanowire: Super P: PTFE binder=8:1:1 (mass ratio), where V_2O_5 nanowire was synthesized similar to the method used previously [12], and Ni foam was used as the current collector. Whatman glass fiber (GF/C) was selected as the separator. Al metal foil (99.9999% Al purity) was used as the counter and reference electrodes, $AlCl_3$/[BMIM]Cl ionic liquids with different mole ratio served as the electrolytes.

Measurements and characterizations

Vibrations of the as-prepared ionic liquids were characterized by Fourier Transform Infrared Spectroscopy (FTIR, Nicolet iS10) at 4 cm^{-1} resolution, by placing a small droplet ionic liquid on the top of a KBr tablet. Cyclic Voltammetry (CV) and ionic conductivity were both measured on CHI604D electrochemical workstation. In CV measurements, glassy carbon electrode (diameter 2mm) was used as working electrode, while Al metal foil was used as the counter and reference electrode, at a scan rate of 10mV/s. Galvanostatic electrochemical charge–discharge cycling of the coin cells were performed on a LAND CT2001A battery tester, under a potential window of 2.5–0.02 V, with a constant current density of 10 mA/g. The morphologies of Al metal foils immerse in $AlCl_3$/[BMIM]Cl ionic liquids for 24h with different mole ratio were examined by using a field-emission scanning electron microscope (FE-SEM QUANTA 6000).

Theoretical calculations

In our approach, compositions of ionic liquids were considered as isolated ion-pairs model in vacuum[31, 32]. Gaussian 09 software[33], with Density Functional Theory (DFT) method at the B3LYP/6-31+G(d, p) theory level was used to optimize conformation, calculate the highest occupied molecular orbital (HOMO) and the lowest unoccupied molecular orbital (LUMO) energies of ion pair models. Mixed basis were used for $[BMIM]^+$-$[AlCl_3I]^-$ ion-pair, in which 6-31+G(d, p) basis was used for C, N, H, Al, Cl atoms, while LanL2DZ basis was used for I atom. Holomb et al[32] found that at least four $[BMIM]^+$ configurations coexisted at room temperature. As for ionic liquids composed of cation and anion, Katsyuba et al[31] found that multiple stable structures are determined with the anion positioned: (a) near to the C_2 atom of the imidazolium ring, (b) between N_1 and C_5, (c) between N_3 and C_4, and (d) between C_4 and C_5. The chemical structures of $[BMIM][AlCl_3X]$ (X=Cl, Br, I) are shown in Fig. 1. Chloride anions in vacuum also occupy positions above or below the imidazolium ring. The position and the type of the anion influence the conformation of the side chains bound to the imidazolium N_1 atom. Vibrations of the cations depend both on the conformational changes and the association with the anion. Thus the ionic liquid was considered to be a mix of cation conformers and mix of ion pairs as well. Considering one of the conformations as the dominant, the others as minor forms, we chose the most stable conformation for analysis.

Results and discussion

Effect of different halogen ions on structure and electrochemical properties of ionic liquids

$AlCl_3$ based ionic liquids are often prepared by binary mixtures of organic halides with $AlCl_3$. The ionic liquids selected here for detailed study are composed of 1-butyl-3-methylimidazolium halides ([BMIM]Cl, [BMIM]Br and [BMIM]Cl) and $AlCl_3$. Considering the properties of the ionic liquids are dependent on their structures, the interactions between the anions and cations are evaluated by infrared spectroscopy.

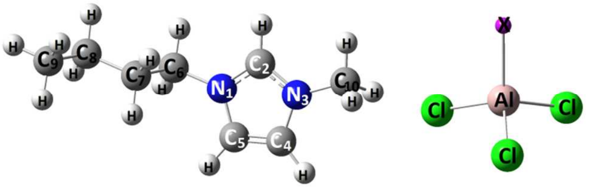

Fig. 1 The chemical structure of the cation and anion components of $[BMIM][AlCl_3X]$(X=Cl, Br, I).

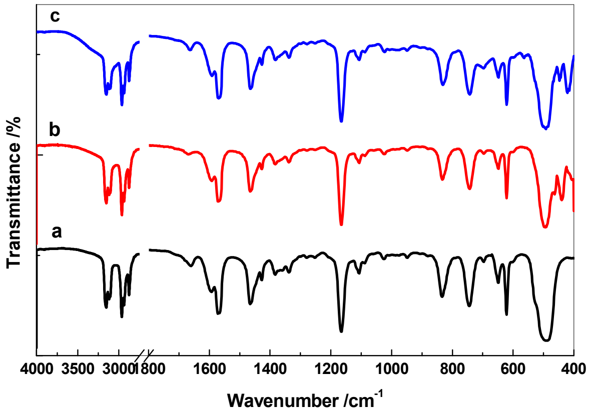

Fig. 2 FTIR spectra of (a) $AlCl_3$/[BMIM]Cl; (b)$AlCl_3$/[BMIM]Br; (c) $AlCl_3$/[BMIM]I ionic liquids

Three kinds of ionic liquids ($AlCl_3$/[BMIM]Cl, $AlCl_3$/[BMIM]Br and $AlCl_3$/[BMIM]I) are investigated to show the effect of halogen anions, where the mole ratio of $AlCl_3$ to halogenated imidazole salt is fixed at 1:1. FTIR spectra of the ionic liquids are displayed in Fig. 2, FTIR vibration modes and the correspondent peak positions are listed in Table 1. Al-Cl, Al-Br, and Al-I stretching vibration are found at 490 cm^{-1}, 440 cm^{-1}, 421cm^{-1}, respectively. According to the FTIR spectra and mole ratio ($AlCl_3$: halogenated imidazole salt =1:1), it can be concluded that $AlCl_4^-$, $AlCl_3Br^-$ and $AlCl_3I^-$ anions exist in these three ionic liquids respectively. The FTIR spectra of the three ionic liquids are very similar above 600 cm^{-1}, because they have the same cations. But a few differences can be detected from the presence of different anions as expected. It is noticed that peak shifts of the ring vibrations are more sensitive, and the side-chain vibrations are seldom affected by the anions. There is a red-shift of vibration modes on imidazole ring with increasing halogen atomic number. The $C_{4,5}$–H and C_2-H stretching vibrations of $AlCl_3$/[BMIM]Cl at 3152, 3119cm^{-1} shift to 3151, 3118cm^{-1} and 3150, 3116cm^{-1} for $AlCl_3$/[BMIM]Br and $AlCl_3$/[BMIM]I, respectively. These shifts are caused by different electronegativity impact of halogen ions. Red-shift implies lower stability of the cations, which further influences the electrochemical windows. It is worth noting that the shift of C_2-H vibration is larger than that of $C_{4,5}$-H, which is probably affected by the position of anions.

To better understand the ion-ion interactions and provide detail information on structure of anions and cations, optimized conformations and the calculated band length of ion pairs are shown in Fig. 3. Al^{3+} is found form complexes with halogen ions near C_2-H, leads to the larger FTIR peak shift of C_2-H than $C_{4,5}$-H, which is consistent with the phenomenon in Fig.2. Al-I bond is the longest (2.5646Å), followed by Al-Br bond (2.2799Å), finally Al-Cl bond (2.1310Å). Since long bond length can result in less stable structure, the stability order of these anions is as follows: $AlCl_3I^-$ < $AlCl_3Br^-$ < $AlCl_4^-$, which is crucial to the electrochemical windows, and will be confirmed in the following tests. In addition, the bond lengths of C-H on imidazole ring have obvious changes, under the influence of $AlCl_3X$ (X=Cl, Br, I) anions located near the C_2 atom of the imidazolium ring. Namely, compared with single $[BMIM]^+$ cation, C_2-H bond in ion pairs becomes longer, while C_4-H and C_5-H bond become shorter. It is consistent with FTIR results in which stretching frequency of $C_{4,5}$ is higher than C_2 in spectra. Overall, there are no significant structure changes of cations.

Table 1 FTIR vibration modes and the correspondent peak positions of ionic liquids

Vibration modes	$AlCl_3$/[BMIM]Cl	$AlCl_3$/[BMIM]Br	$AlCl_3$/[BMIM]I
$C_{4,5}$-H stretching	3152	3151	3150
C_2-H stretching	3119	3118	3116
CH_3 asymmetric stretching	2963	2963	2961
CH_2 asymmetric stretching	2937	2936	2936
CH_3 symmetric stretching	2876	2876	2875
C=C stretching	1661	1668	1663
C=N stretching	1593	1592	1591
	1571	1570	1570
CH_3 asymmetric bending	1465	1465	1464
CH_2 in plane bending	1428	1428	1427
CH_3 symmetric bending	1383	1383	1382
CH_2 out plane bending	1338	1338	1337
C_2-H in-plane deformation	1166	1166	1166
$C_{4,5}$-H in-plane deformation	1107	1107	1107
Ring in-plane deformation	1024	1024	1023
Ring CH_2 rocking	948	948	948
C_2-H out-plane deformation	833	832	831
$C_{4,5}$-H out-plane deformation	744	743	743
Ring out-plane deformation	649	649	648
	621	621	621
Al-Cl stretching	490	494	492
Al-Br stretching		440	
Al-I stretching			421

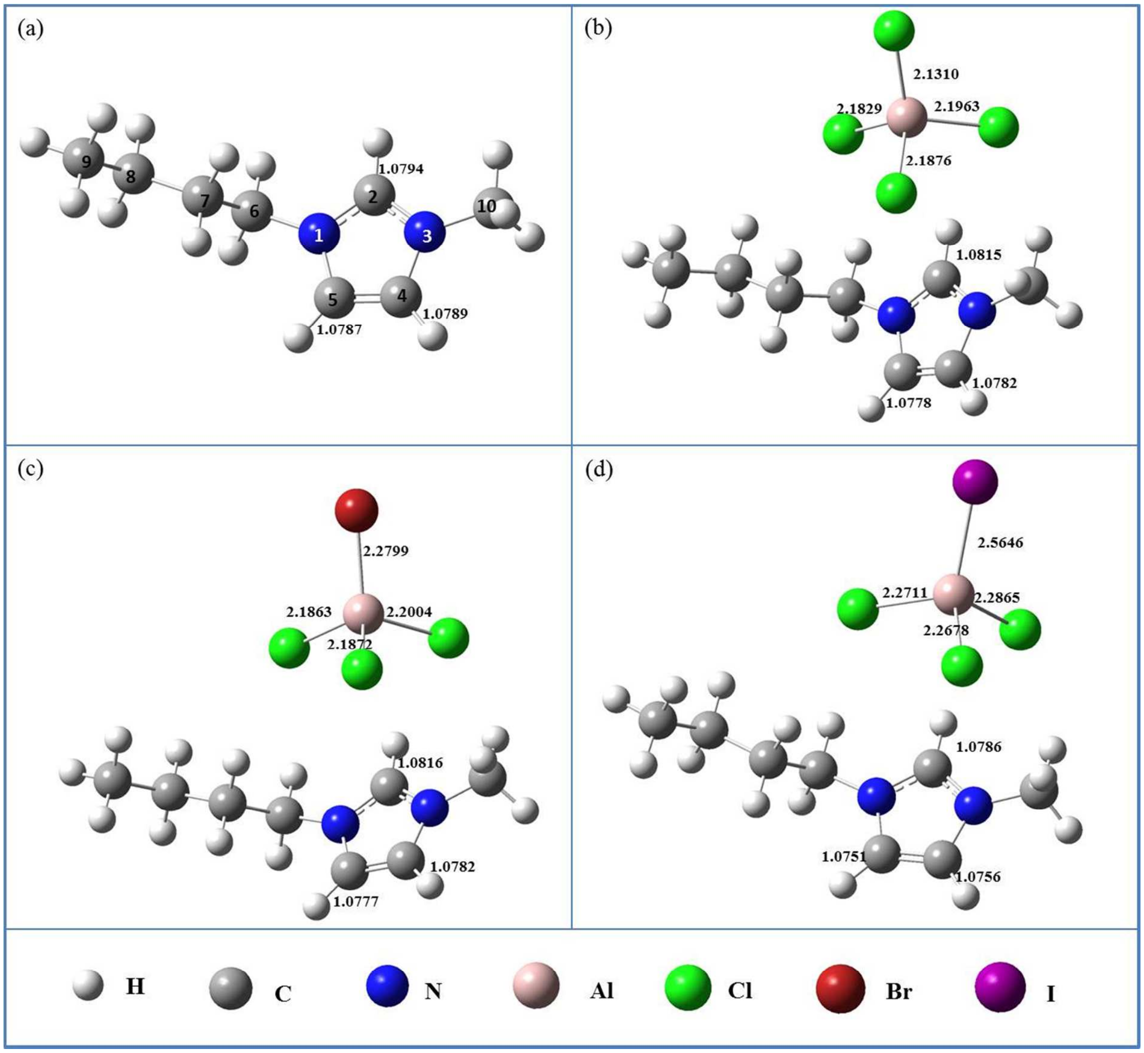

Fig. 3 The energetically preferred conformation of (a) $[BMIM]^+$; (b) $[BMIM]^+$-$[AlCl_4]^-$; (c) $[BMIM]^+$-$[AlCl_3Br]^-$; (d) $[BMIM]^+$-$[AlCl_3I]^-$ from the DFT calculations

In order to understand the effect on electrochemical properties caused by different anions, electrochemical window and conductivity of the ionic liquids are investigated, as shown in Fig. 4. Since Al is used as quasi-reference electrode, the potential in the voltammogram is often denoted as V vs. Al/Al^{3+}. The cathodic limiting potentials of ionic liquids correspond to the reduction potential of imidazole ring, and are at –2.1 V (vs. Al/Al^{3+}) in $AlCl_3$/[BMIM]Cl, –1.9 V (vs. Al/Al^{3+}) in $AlCl_3$/[BMIM]Br and -1.0V (vs. Al/Al^{3+}) in $AlCl_3$/[BMIM]I. While the anodic limiting potentials are at 2.6V (vs. Al/Al^{3+}) for $AlCl_3$/[BMIM]Cl ionic liquids, followed by $AlCl_3$/[BMIM]Br (2V vs. Al/Al^{3+}), and finally the $AlCl_3$/[BMIM]I (1V vs. Al/Al^{3+}). Shifts of cathodic and anodic limiting potential are consistent with structure analysis above. Larger halogen atom related to lower stabilities of cations and anions. The anodic limiting reactions of ionic liquids are as follows:

$$4AlCl_4^- - 2e^- \rightarrow Cl_2 + 2Al_2Cl_7^- \quad (1)$$

$$4AlCl_3Br^- - 2e^- \rightarrow Br_2 + 2Al_2Cl_6Br^- \quad (2)$$

$$4AlCl_3I^- - 2e^- \rightarrow I_2 + 2Al_2Cl_6I^- \quad (3)$$

In electrolytes, the anodic limiting potential determines the voltage window of the rechargeable aluminum battery. $AlCl_3$/[BMIM]Cl has a much higher electrochemical window (4.7V) than $AlCl_3$/[BMIM]Br (3.9V) and $AlCl_3$/[BMIM]I (2V), which is more promising to be used in rechargeable aluminum battery.

The conductivities for all these ionic liquids increase with increasing temperature, as shown in Fig. 4b. Bonhôte used the Stokes–Einstein relation to derive an expression for the conductivity of charge in ionic liquids[34]:

$$\kappa = \frac{yK^2\rho}{(6\pi N_A M_W \eta)}[(\xi_+R_+)^{-1} + (\xi_-R_-)^{-1}] \quad (4)$$

where y is the degree of dissociation, F is the Faraday constant, ρ is the density, M_W is the molar mass of the ionic liquid, N_A is the Avogadro constant, η is viscosity, ξ_+ and ξ_- are correction factors to take into account specific interactions between the mobile ions in the melt, R_+ and R_- are the radii of the cation and anion.

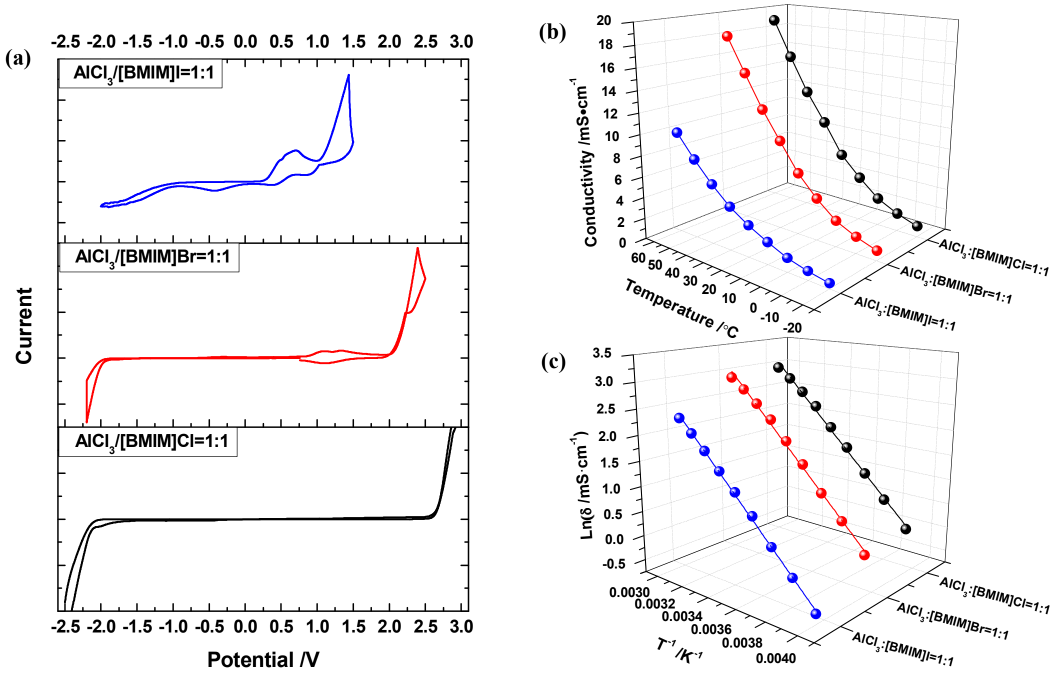

Fig. 4 Comparison of the electrochemical window and conductivity of different ionic liquids.(a) Cyclic voltammogram; (b) Conductivity-temperature (δ-T) curves; (c) Arrhenius Fitted curves of ionic liquids

The increasing temperature leads to viscosity reduction, which further results in enhanced conductivity. According to equation (4), the conductivity is reduced with the increasing radii of anion, which is confirmed by the experimental results. Namely, $AlCl_3$/[BMIM]Cl ionic liquid has a higher conductivity (9.1 mS/cm, 30℃) than $AlCl_3$/[BMIM]Br (8.6 mS/cm, 30℃) and $AlCl_3$/[BMIM]I (4.3 mS/cm, 30 ℃). The conductivity–temperature relationship follows Arrhenius formula, as shown in Fig. 4c. Thus, it can be concluded that ionic liquid composed entirely of chloroaluminate anion has the highest oxidation potential, widest electrochemical window, and highest conductivity among all the halogenated aluminum containing ionic liquids in this work. The conductivity of $AlCl_3$/[BMIM]Cl (9.1 mS/cm, 30℃) is high enough to be used as electrolyte in rechargeable aluminum batteries.

Theory calculation can also help to analyze and predict the electrochemical properties of the ionic liquids. Charge distribution and energy level of $[BMIM]^+$-$[AlCl_4]^-$, $[BMIM]^+$-$[AlCl_3Br]^-$ and $[BMIM]^+$-$[AlCl_3I]^-$ ion-pairs calculated by DFT are shown in Fig. 5. The thermochemical corrections are scaled by using the factor of 0.9806 for the B3LYP/6-31G+(d) model chemistry[35]. As shown in Fig. 5, HOMO is distributed on the anions, while LUMO is distributed on the cations in these ion pairs. That is to say, HOMO is dominated by the anion states， while the LUMO is dominated by the cation states. Therefore, the anodic limiting potential of the ionic liquids is determined by the oxidation of the anions, while the cathodic limiting potential is determined by reduction of the cations. It is worth noting that the atoms on imidazole ring of $[BMIM]^+$ make major contributions to LUMO level, which means side chains have less impact on cathodic limiting potential.

Among these ion pairs, $[BMIM]^+$-$[AlCl_4]^-$ shows the lowest HOMO energy, followed by $[BMIM]^+$-$[AlCl_3Br]^-$, finally $[BMIM]^+$-$[AlCl_3I]^-$. Lower HOMO energy means higher oxidation stability. Thus, $[BMIM]^+$-$[AlCl_4]^-$ displays the highest oxidative decomposition voltage and widest electrochemical window, as shown in Fig. 4a. Considering a vast combination of available cations and anions that can be used to synthesize ionic liquids, adopting theoretical approaches to predict and accurate tailor properties of ionic liquids is crucial to further enhance the performance of electrochemical devices[36].

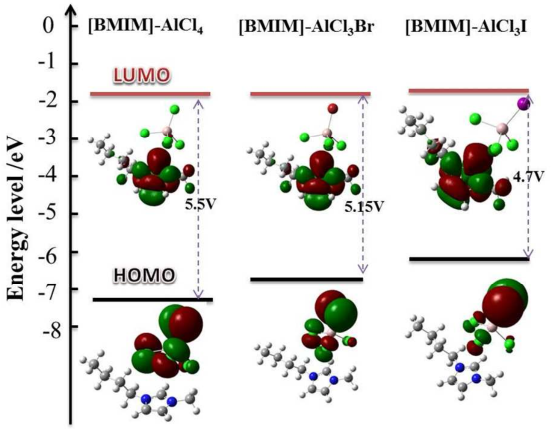

Fig. 5 HOMO and LUMO plots of $[BMIM]^+$-$[AlCl_4]^-$, $[BMIM]^+$-$[AlCl_3Br]^-$, $[BMIM]^+$-$[AlCl_3I]^-$ calculated by DFT

Effect of different $AlCl_3$ mole fraction on structure and electrochemical properties of ionic liquids

According to the above analysis, ionic liquid synthesized by imidazolium chloride and $AlCl_3$ shows the best electrochemical performance. However, the most significantly feature of $AlCl_3$ containing ionic liquid system, with difference from other nonchloroaluminate systems, is that its compositions changed with the mole ratio of $AlCl_3$ in halogenated imidazole salt. Thus, it is essential to clarify the structure and electrochemical property of these ionic liquids with different $AlCl_3$ ratio for use of rechargeable aluminum battery electrolyte.

FTIR spectra of $AlCl_3$/[BMIM]Cl ionic liquids with different mole ratio are shown in Fig. 6. The vibration modes and the correspondent peak positions are listed in Table 2. It can be seen that the vibration intensity of Al-Cl bond at 490 cm^{-1} increase with $AlCl_3$:[BMIM]Cl mole ratio. When this mole ratio is higher than 1:1, the peak at 440cm^{-1} emerges, and becomes stronger with increasing mole ratio, which is attributed to the vibration of Al-Cl-Al bond in $Al_2Cl_7^-$ or larger chloroaluminate species. Meanwhile, increasing $AlCl_3$ content means the emergence of a larger chloroaluminate complexes anions ($AlCl_4^- \rightarrow Al_2Cl_7^- \rightarrow Al_3Cl_{10}^- \rightarrow$…), which affects the vibrations of $[BMIM]^+$ and subsequently lead to the decrease of peak intensity. In addition, with increasing $AlCl_3$:[BMIM]Cl mole ratio, C-H and imidazole ring out-plane deformation have red-shift, while ring in-plane deformation has a blue-shift. It is worth noting that C_2-H stretching frequency (3116cm^{-1}) of $AlCl_3$/[BMIM]Cl=0.8:1 is lower than that of other ionic liquids (3119cm^{-1}), which is attributed to the existence of Cl^-.

Table 2 FTIR vibration modes and the correspondent peak positions of $AlCl_3$/[BMIM]Cl ionic liquids with different mole ratio ($AlCl_3$:[BMIM]Cl)

Vibration modes	0.8:1	1:1	1.1:1	1.5:1	2:1
$C_{4,5}$-H stretching	3152	3152	3152	3152	3153
C_2-H stretching	3116	3119	3119	3119	3119
CH_3 asymmetric stretching	2962	2963	2963	2963	2964
CH_2 asymmetric stretching	2937	2937	2937	2937	2937
CH_3 symmetric stretching	2876	2876	2876	2876	2877
C=C stretching	1661	1661	1672	1666	1666
	1593	1593	1594	1594	1594
C=N stretching	1571	1571	1571	1571	1566
CH_3 asymmetric bending	1465	1465	1465	1465	1465
CH_2 in plane bending	1428	1428	1428	1428	1428
CH_3 symmetric bending	1383	1383	1383	1384	1385
CH_2 out plane bending	1338	1338	1338	1337	1338
C_2-H in-plane deformation	1166	1166	1166	1165	1165
$C_{4,5}$-H in-plane deformation	1107	1107	1107	1107	1107
Ring in-plane deformation	1021	1024	1025	1030	1027
Ring CH_2 rocking	948	948	948	948	948
C_2-H out-plane deformation	833	833	833	832	832
$C_{4,5}$-H out-plane deformation	746	744	744	743	743
Ring out-plane deformation	650	649	649	648	648
	622	621	621	621	621
Al-Cl stretching	492	490	497	492	492
			440	443	440

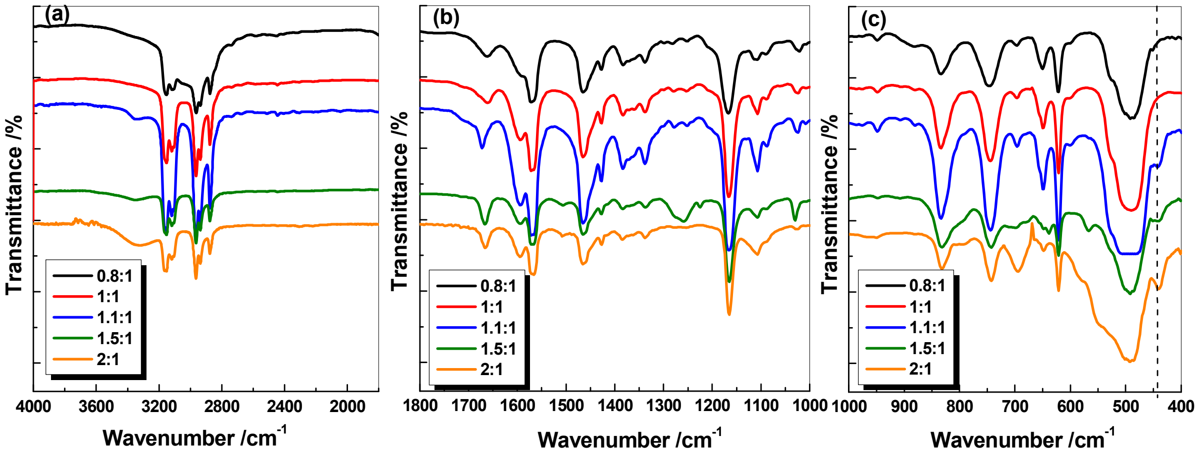

Fig. 6 FTIR spectra of $AlCl_3$/[BMIM]Cl ionic liquids with different mole ratio (a) 4000-1800 cm^{-1}; (b) 1800-1000 cm^{-1}; (c)1000-400 cm^{-1}.

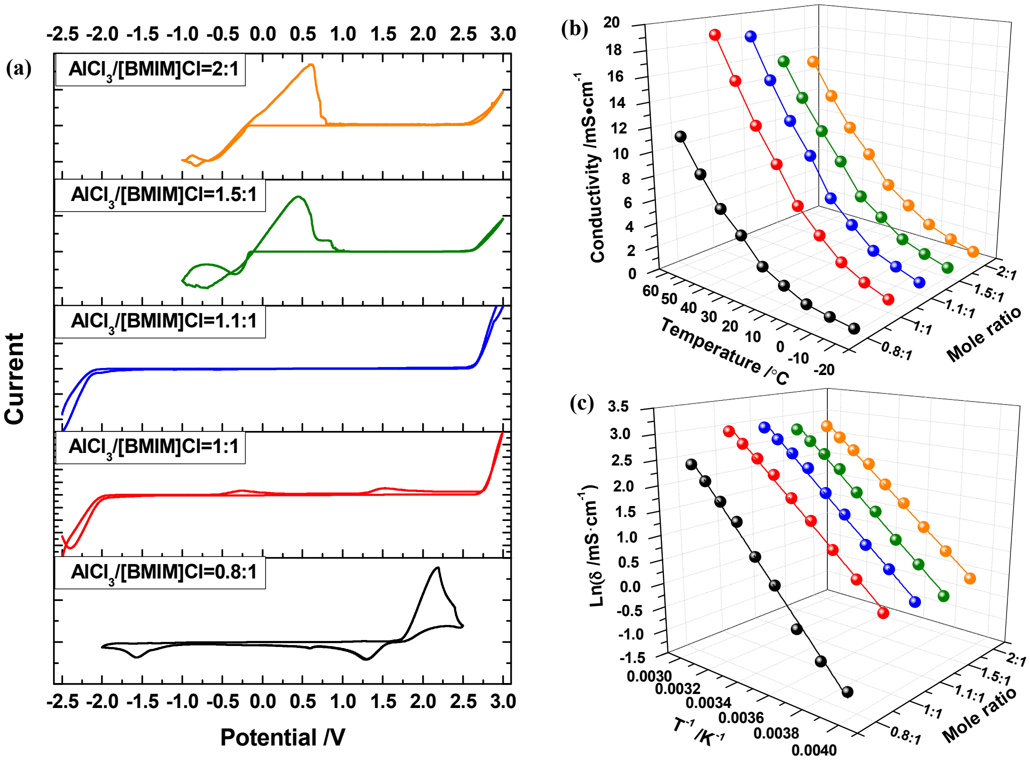

Fig. 7 (a) Cyclic voltammogram; (b) Conductivity-temperature (δ-T) curves; (c) Arrhenius Fitted curves of $AlCl_3$/[BMIM]Cl ionic liquids.

It can be seen from Fig. 7a that anode limiting potentials of $AlCl_3$/[BMIM]Cl ionic liquids are about 2.6 V (vs Al/Al^{3+}), when $AlCl_3$:[BMIM]Cl mole ratio are 1:1, 1.1:1, 1.5:1 and 2:1, higher than that of $AlCl_3$/[BMIM]Cl=0.8:1(1.75 V). Great differences also reflect in cathode limiting potential. It is about -0.2V (vs Al/Al^{3+}) at $AlCl_3$:[BMIM]Cl mole ratio 1.5:1 and 2:1, which is much higher than that (-2.0V vs Al/Al^{3+}) of low $AlCl_3$:[BMIM]Cl mole ratio (0.8:1, 1:1 and 1.1:1). Corresponding electrochemical windows of the ionic liquids at different $AlCl_3$:[BMIM]Cl mole ratio are 3.75V for 0.8:1, 4.6V for 1:1 and 1.1:1, 2.8V for 1.5:1 and 2:1. This result is caused by the difference of anion compositions in the ionic liquids. When

$AlCl_3$:[BMIM]Cl mole ratio is less than 1:1, namely 0.8:1, Cl^- and $AlCl_4^-$ coexist, the ionic liquid is basic; when mole ratio exactly equals to 1:1, only $AlCl_4^-$ exists, in this case the ionic liquid is neutral; when mole ratio is higher than 1:1, $Al_2Cl_7^-$ or larger complex anions appear, the ionic liquid becomes acidic. Lewis acidity of chloroaluminate ionic liquid is determined by chloride activity according to equation (5)[37-39]:

$$2AlCl_4^- \rightarrow Al_2Cl_7^- + Cl^- \quad (5)$$

Anodic limiting reactions when $AlCl_3$:[BMIM]Cl mole ratio equals to 1:1 is shown in equation (1), while corresponding oxidation reactions with a mole ratio higher or less than 1:1 are as follows[39]:

$$6Al_2Cl_7^- - 2e^- \rightarrow Cl_2 + 4Al_3Cl_{10}^- \quad (6)$$

$$2Cl^- - 2e^- \rightarrow Cl_2 \quad (7)$$

Cathode limiting reaction is corresponding to an irreversible reduction associated with the organic cation in ionic liquids with mole fraction lower than 1.5:1. A pair of strong redox peaks appears around 0 V when $AlCl_3$:[BMIM]Cl mole ratio is higher than 1.5:1, with increasing current intensity. This phenomenon may be explained as electrochemical reduction of the adsorbed $[BMIM]^+$ and subsequent oxidation[40], along with the redox of $Al_2Cl_7^-$, as reported previously[38, 41]:

$$4Al_2Cl_7^- + 3e^- \rightarrow Al + 7AlCl_4^- \quad (8)$$

It is interesting that the electrochemical activity of $[BMIM]^+$ in ionic liquid at high $AlCl_3$:[BMIM]Cl (1.5:1 and 2:1) is increased, which lead to the positive shift of cathodic limiting potential.

Conductivities of $AlCl_3$/[BMIM]Cl ionic liquids at different temperatures are shown in Fig. 7b. All the ionic liquids exhibit the conductivity of the order of 10^{-3} S cm^{-1} at room temperature and 10^{-2} S cm^{-1} at ~60 °C, showing an excellent property for potential application in rechargeable aluminum batteries for wide temperature range. The ionic liquid has the highest conductivity when $AlCl_3$:[BMIM]Cl mole ratio is 1:1, then conductivity decreases with increasing mole ratio. The conductivity–temperature plots meet with Arrhenius (Fig. 7c).

Impact of anions composition and concentration on rechargeable aluminum battery performance

Now it is clear that the anions in $AlCl_3$:[BMIM]Cl have a great impact on the electrochemical properties of the ionic liquids, which are very likely further affect the performances of rechargeable aluminum batteries. The composition of the ionic liquids are also considered to affect over potential of Al deposition, in turn affect the size of the particles of aluminum deposition[42]. Thus charge/discharge performances of rechargeable aluminum batteries using $AlCl_3$/[BMIM]Cl ionic liquids as electrolyte are investigated, where V_2O_5 nanowire is used as cathode material.

Initial discharge profiles of rechargeable aluminum batteries using $AlCl_3$/[BMIM]Cl ionic liquids with different mole ratio are show in Fig. 8a, where the inset is the local magnification of discharge profiles. All these batteries can't be charged, except the one using ionic liquid at mole ratio 1.1:1. In addition, the batteries using $AlCl_3$/[BMIM]Cl ionic liquid with the mole ratios of 1.5:1 and 2:1 have a discharge capacity about 152 mAh/g and 110 mAh/g respectively; while those using $AlCl_3$/[BMIM]Cl ionic liquid with the mole ratio of 0.8:1 and 1:1 have no electrochemical activity. Cells using ionic liquids with high $AlCl_3$ mole fraction cannot be charged is probably due to the electrochemical activity of organic cations at potential close to the aluminum reduction-oxidation process in these ionic liquids. Charge/discharge profiles of the battery with $AlCl_3$/[BMIM]Cl=1.1:1 are shown in Fig. 8b. It has high discharge voltage platform (1 V) and high capacity (288 mAh/g) at the first cycle, followed by the steady discharge voltage platform at 0.5 V and charge voltage platform at 1.0 V. Its charge and discharge capacities are stabilized at 140mAh/g and 130mAh/g in the 5th cycle, respectively. The initial discharge curve has a higher voltage platform and capacity compared to the following cycles. The intercalated Al atoms may be partially trapped in the V_2O_5 crystal lattice after the first cycle[20]. The high valence of Al^{3+} in host materials may block the ion mobility[21], which leads to a large polarization and capacity fading in the following cycles.

To reveal the impact of ionic liquid on anode of rechargeable aluminum battery, Al metal foils immersed in $AlCl_3$/[BMIM]Cl ionic liquids with different mole ratio for 24 h, and the SEM images after immersing are shown in Fig. 9. Varying degrees of corrosion are observed Al metal foil surface. No corrosion is found on Al metal foil surface when mole ratio of $AlCl_3$/[BMIM]Cl ionic liquids is not exceeding 1:1. Pitting corrosion begin to occur on Al metal foil surface when mole ratio is 1.1:1, while severe corrosion appears on Al metal foil surfaces when mole ratio are 1.5:1 and 2:1. Corrosion extent increases with increasing $AlCl_3$:[BMIM]Cl mole ratio. As discussed in the FTIR spectra, $Al_2Cl_7^-$ anions only exist when $AlCl_3$:[BMIM]Cl mole ratio exceeds 1:1, and will further increase with higher $AlCl_3$:[BMIM]Cl mole ratio. Thus, the active $Al_2Cl_7^-$ anions lead to the occurrence of corrosion.

It is known that aluminum can only be deposited from the acid melt which contained $Al_2Cl_7^-$, for $AlCl_4^-$ in basic and neutral melt has a highly symmetric tetrahedral structure and the electrochemical activity is poor[34]. $Al_2Cl_7^-$ in acid ionic liquid is considered act as electrochemical active material in Al(III) reduction at anode. It explains why the batteries use basic ($AlCl_3$:[BMIM]Cl=0.8:1) and neutral ($AlCl_3$:[BMIM]Cl=1:1) ionic liquids can't be charged/discharged. $AlCl_3$/[BMIM]Cl ionic liquid with lower $Al_2Cl_7^-$ concentration ($AlCl_3$:[BMIM]Cl=1.1:1) cause slightly corrosion on Al anode surfaces, which can help removing the oxide film on Al surface, thus results in the best charge and discharge performance. However, the $AlCl_3$/[BMIM]Cl ionic liquids with higher $Al_2Cl_7^-$ concentration ($AlCl_3$:[BMIM]Cl=1.5:1 and 2:1) have extremely high activities, which cause severe corrosion of Al anode, and even result in corrosion of collector and battery shell, as well as other side reactions, therefore can't show satisfying electrochemical performances. That is to say, the excellent performance of the battery using $AlCl_3$/[BMIM]Cl=1.1:1 ionic liquid is attributed to the appropriate $Al_2Cl_7^-$ concentration.

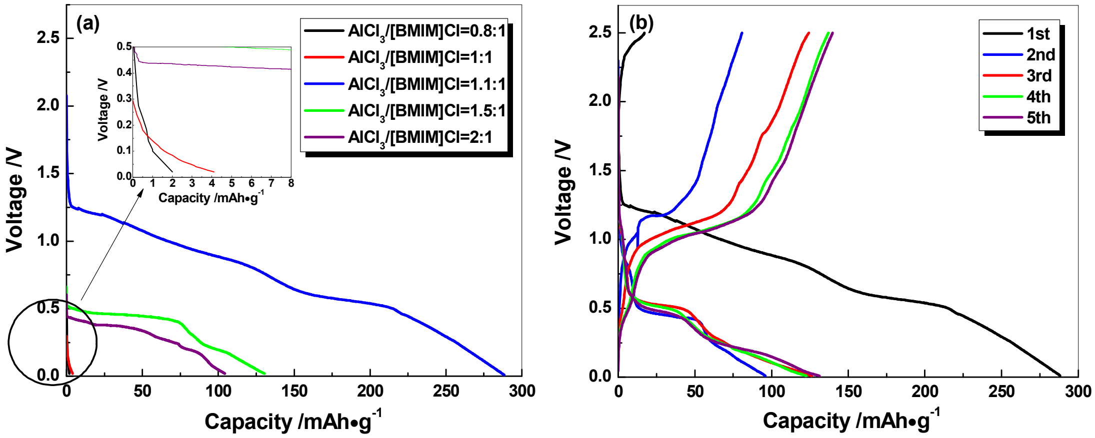

Fig. 8 (a) Initial discharge profiles of rechargeable aluminum batteries using $AlCl_3$/[BMIM]Cl ionic liquids with different mole ratio; (b)Charge/discharge profiles of rechargeable aluminum battery using $AlCl_3$/[BMIM]Cl=1.1:1 ionic liquid.

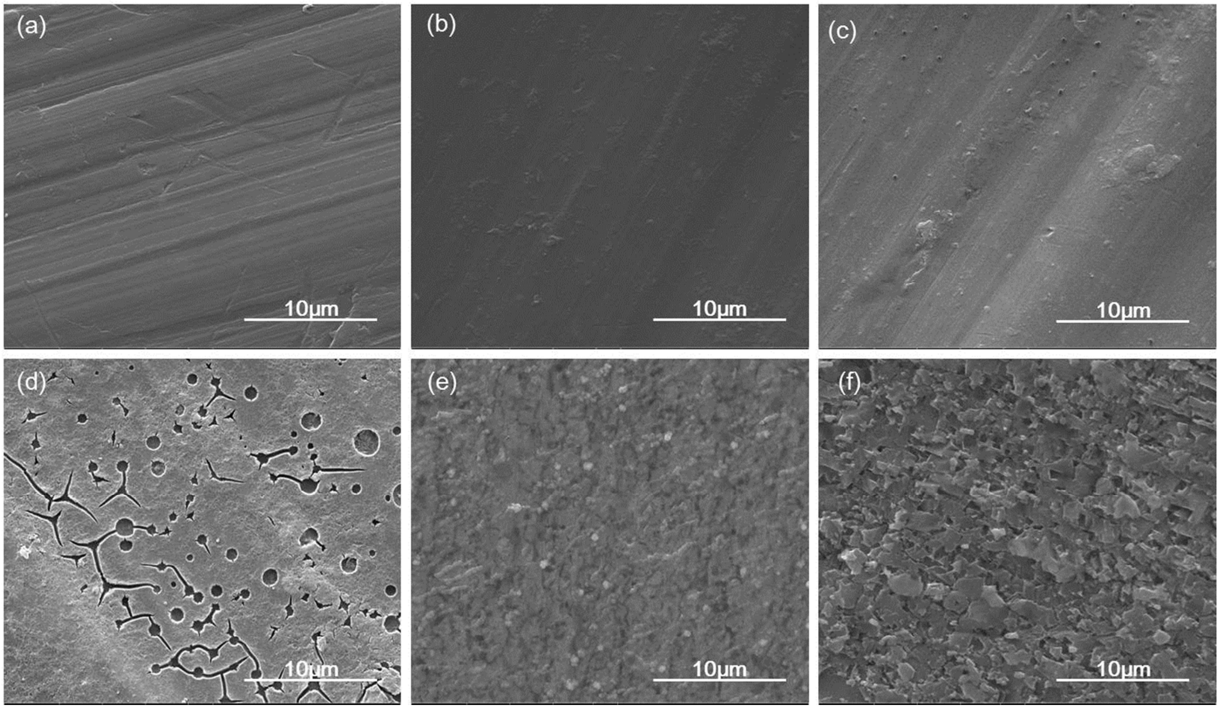

Fig. 9 SEM images of Al metal foils immerse in $AlCl_3$/[BMIM]Cl ionic liquids with different mole ratio for 24h: (a) initial; (b) 0.8:1; (c) 1:1; (d) 1.1:1; (e) 1.5:1; (f) 2:1

Conclusions

Ionic liquids prepared by different halogenated imidazole salt and $AlCl_3$/imidazolium chloride mole ratio were investigated. Electrochemical window and conductivity of ionic liquids are affected by the anions, which mainly reflect in two aspects: (1) Halogen anions ($AlCl_4^- \rightarrow AlCl_3Br^- \rightarrow AlCl_3I^-$) result from different halogenated imidazole salt species is the critical factor for the electrochemical windows; (2) Aluminum chloride anions ($Cl^- \rightarrow AlCl_4^- \rightarrow Al_2Cl_7^-$) result from different AlCl3/imidazole salt mole ratio is the determinate of the electrochemical activities. Theoretical calculation is adopted to help analyze structure and electrochemical properties of ionic liquids. Charge/discharge performance of rechargeable aluminum batteries using $AlCl_3$/[BMIM]Cl ionic liquids as electrolyte and V_2O_5 nanowire as cathode was investigated. Different charge/discharge performance is found in these batteries, where the concentration of $Al_2Cl_7^-$ is considered as a key factor. For the battery using $AlCl_3$/[BMIM]Cl=1.1:1 ionic liquid as electrolyte , a proper $Al_2Cl_7^-$ concentration result in a slightly pitting corrosion on Al metal anode, which can help wiping off the oxide film on Al metal foil and improve the charge/discharge performance. Namely, it achieves a high capacity of 288 mAh/g at the initial cycle, which is corresponding to a two-electron reaction. In conclusion, this work aims to reveal anion-effect on ionic liquid properties and rechargeable aluminum battery performance. It is expected to provide guidance on how to design and select proper electrolytes of rechargeable aluminum batteries.

Acknowledgements

The present work is supported by the National Basic Research Program of China (Grant No. 2015CB251100), the Program for New Century Excellent Talents in University (Grant No. NCET-13-0033), and the Beijing Co-construction Project (Grant No. 20150939014).

References

1 V. Palomares, P. Serras, I. Villaluenga, K. B. Hueso, J. Carretero-Gonzalezb and T. Rojo, *Energy Environ. Sci.*, 2012, **5**, 5884–5901.

2 H. Pan, Y.-S. Hu and L. Chen, *Energy Environ. Sci.*, 2013, **6**, 2338-2360.

3 M. D. Slater, D. Kim, E. Lee and C. S. Johnson, *Adv. Funct. Mater.*, 2013, **23**, 947–958.

4 Y. Bai, Z. Wang, C. Wu, R. Xu, F. Wu, Y. Liu, H. Li, Y. Li, J. Lu and K. Amine, *ACS Appl. Mater. Interfaces*, 2015, **7**, 5598-5604.

5 H. Li, Y. Bai, F. Wu, Y. Li and C. Wu, *J. Power Sources*, 2015, **273**, 784-792.

6 H. Li, X. Yu, Y. Bai, F. Wu, C. Wu, L.-Y. Liua and X.-Q. Yang, *J. Mater. Chem. A*, 2015, **3**, 9578–9586.

7 D. Aurbach, Z. Lu, A. Schechter, Y. Gofer, H. Gizbar, R. Turgeman, Y. Cohen, M. Moshkovich and E. Levi, *Nature*, 2000, **407**, 724-727.

8 D. Aurbach, I. Weissman, Y. Gofer and E. Levi, *Chem. Rec.*, 2003, **3**, 61-73.

9 T. D. Gregory, R. J. Hoffman and R. C. Winterton, *J. Electrochem. Soc.*, 1990, **137**, 775-780.

10 P. Saha, M. K. Datta, O. I. Velikokhatnyi, A. Manivannan, D. Alman and P. N. Kumta, *Prog. Mater Sci.*, 2014, **66**, 1-86.

11 Y. Orikasa, T. Masese, Y. Koyama, T. Mori, M. Hattori, K. Yamamoto, T. Okado, Z.-D. Huang, T. Minato, C. d. Tassel, J. Kim, Y. Kobayashi, T. Abe, H. Kageyama and Y. Uchimoto, *Sci. Rep.*, 2014, 1-6.

12 N. Jayaprakash, S. K. Das and L. A. Archer, *Chem. Comm.*, 2011, **47**, 12610-12612.

13 L. D. Reed and E. Menke, *J. Electrochem. Soc.*, 2013, **160**, A915-A917.

14 W. Wang, B. Jiang, W. Xiong, H. Sun, Z. Lin, L. Hu, J. Tu, J. Hou, H. Zhu and S. Jiao, *Sci. Rep.*, DOI:10.1038/srep03383 (2013).

15 J. V. Rani, V. Kanakaiah, T. Dadmal, M. S. Rao and S. Bhavanarushi, *J. Electrochem. Soc.*, 2013, **160**, A1781-A1784.

16 H. Wang, Y. Bai, S. Chen, X. Luo, C. Wu, F. Wu, J. Lu and K. Amine, *ACS Appl. Mater. Interfaces*, 2015, **7**, 80-84.

17 S. Liu, J. J. Hu, N. F. Yan, G. L. Pan, G. R. Li and X. P. Gao, *Energy Environ. Sci.*, 2012, **5**, 9743-9746.

18 Y. J. He, J. F. Peng, W. Chu, Y. Z. Lia and D. G. Tong, *J. Mater. Chem. A*, 2014, **2**, 1721–1731.

19 M.-C. Lin, M. Gong, B. Lu, Y Wu, D.-Y. Wang, M. Guan, M. Angell, C. Chen, J. Yang, B.-J. Hwang and H. Dai, *Nature*, 2015, 1-6.

20 L. Geng, G. Lv, X. Xing and J. Guo, *Chem. Mater.*, 2015, **27**, 4926-4929.

21 S. Liu, G. L. Pan, G. R. Li and X. P. Gao, *J. Mater. Chem. A*, 2015, **3**, 959–962.

22 L. D. Reed, S. N. Ortiz, M. Xiong and E. J. Menke, *Chem. Commun.*, 2015, **51**, 14397-14400.

23 G. Cohn, L. Ma and L. A. Archer, *J. Power Sources*, 2015, **283**, 416-422.

24 Q. Li and N. J. Bjerrum, *J. Power Sources*, 2002, **110**, 1-10.

25 H. Wang, Y. Bai, S. Chen, F. Wu and C. Wu, *Prog. Chem.*, 2013, **25**, 1392-1400.

26 F. Wu and C. Wu, *Chin. Sci. Bull.*, 2014, **59**, 3369–3376.

27 T. Mandai and P. Johansson, *J. Mater. Chem. A*, 2015, **3**, 12230–12239.
28 H. Hu, W. Yuan, Z. Jia and G. L. Baker, *Rsc Adv.*, 2015, **5**, 3135-3140.
29 H. Hu, W. Yuan, L. Lu, H. Zhao, Z. Jia and G. L. Baker, *J. Polym. Sci., Part A: Polym. Chem.*, 2014, **52**, 2104-2110.
30 Z. Jia, W. Yuan, C. Sheng, H. Zhao, H. Hu and G. L. Baker, *J. Polym. Sci., Part A: Polym. Chem.*, 2015, **53**, 1339-1350.
31 S. A. Katsyuba, E. E. Zvereva, A. Vidis and P. J. Dyson, *J. Phys. Chem. A*, 2007, **111**, 352-370.
32 R. Holomb, A. Martinelli, Albinsson, J. C. Lassegues, P. Johansson and P. Jacobsson, *J. Raman Spectrosc.*, 2008, **39**, 793–805.
33 M. J. F. Gaussian 09, G. W. Trucks, H. B. Schlegel, G. E. Scuseria, M. A. Robb, J. R. Cheeseman, G. Scalmani, V. Barone, B. Mennucci, G. A. Petersson, H. Nakatsuji, M. Caricato, X. Li, H. P. Hratchian, A. F. Izmaylov, J. Bloino, G. Zheng, J. L. Sonnenberg, M. Hada, M. Ehara, K. Toyota, R. Fukuda, J. Hasegawa, M. Ishida, T. Nakajima, Y. Honda, O. Kitao, H. Nakai, T. Vreven, J. A. Montgomery, Jr., J. E. Peralta, F. Ogliaro, M. Bearpark, J. J. Heyd, E. Brothers, K. N. Kudin, V. N. Staroverov, R. Kobayashi, J. Normand, K. Raghavachari, A. Rendell, J. C. Burant, S. S. Iyengar, J. Tomasi, M. Cossi, N. Rega, J. M. Millam, M. Klene, J. E. Knox, J. B. Cross, V. Bakken, C. Adamo, J. Jaramillo, R. Gomperts, R. E. Stratmann, O. Yazyev, A. J. Austin, R. Cammi, C. Pomelli, J. W. Ochterski, R. L. Martin, K. Morokuma, V. G. Zakrzewski, G. A. Voth, P. Salvador, J. J. Dannenberg, S. Dapprich, A. D. Daniels, O. Farkas, J. B. Foresman, J. V. Ortiz, J. Cioslowski, and D. J. Fox, Gaussian 09, Revision D.01, Gaussian, Inc., Wallingford CT, 2009.
34 P. Bonhôte, A.-P. Dias, N. Papageorgiou, K. Kalyanasundaram and M. Gra1tzel, *Inorg. Chem.*, 1996, **35**, 1168-1178.
35 A. P. Scott and L. Radom, *J. Phys. Chem.*, 1996, **100**, 16502-16513.
36 E. I. Izgorodina, *Phys. Chem. Chem. Phys.*, 2011, **13**, 4189–4207.
37 Z. J. Karpinskit and R. A. Osteryoung, *Inorg. Chem.*, 1984, **23**, 1491-1494.
38 T. J. Melton, J. Joyce, J. T. Maloy, J. A. Boon and J. S. Wilkes, *J. Electrochem. Soc.*, 1990, **137**, 3865-3869.
39 P. R. Gifford and J. B. Palmisano, *MOLTEN SALT*, 1986, **134**, 610-614.
40 B. Vestergaard, N. J. Bjerrum, I. Petrushina, H. A. Hiuler, R. W. Berg and M. Begtrup, *J. Electrochem. Soc.,* 1993, **140**, 3108-3113.
41 R. T. Carlin, W. Crawford and M. Bersch, *J. Electrochem. Soc.*, 1992, **139**, 2720-2727.
42 D. Pradhan and R. G. Reddy, presented in part at the The Minerals, Metals & Materials Society and ASM International, 2012.

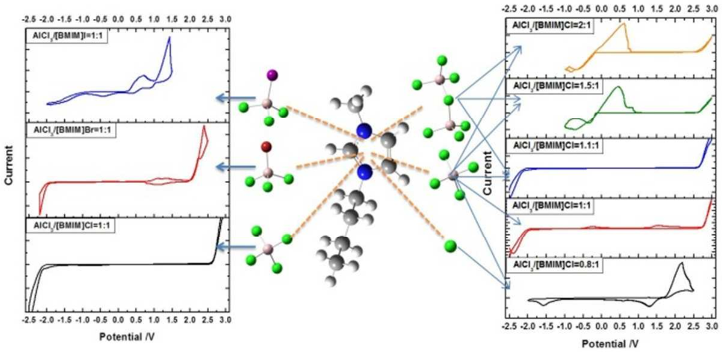

$AlCl_3$-based ionic liquids are designed and used as the electrolytes for rechargeable aluminum batteries, whose electrochemical properties are affected by the anions in two aspects: (1) Halogen anions ($AlCl_4^-$→$AlCl_3Br^-$→$AlCl_3I^-$) result from different halogenated imidazole salt species is the critical factor for the electrochemical windows; (2) Aluminum chloride anions (Cl^-→$AlCl_4^-$→$Al_2Cl_7^-$) result from different AlCl3/imidazole salt mole ratio is the determinate of the electrochemical activities.